Refining the Canegro model for improved simulation of climate change impacts on sugarcane: Model description

Jones M.R. and Singels A.

South African Sugarcane Research Institute, Mount Edgecombe, 4300, South Africa

Corresponding author: Matthew Jones, matthew.jones@sugar.org.za.

Supplementary material to:

Jones, M.R. and Singels, A. 2018. Refining the Canegro model for improved simulation of climate change impacts on sugarcane. *Eur. J. Agron.*

Contents

APPENDIX A DETAILED MODEL DESCRIPTION

A1 Introduction

The main objective of this work was to modify the DSSAT-Canegro v4.5 model (Singels *et al.*, 2008) in order to improve its simulation capabilities for climate change applications. This appendix describes the algorithms that are included in two new versions of the model. Model version numbering is as follows:

- V4.5_C1.0 – The original implementation of the Canegro model (Inman-Bamber, 1991; Singels and Bezuidenhout, 2002) in the DSSAT v4.5 modular Cropping System Model (Jones *et al.*, 2003) framework. This model is described in Singels et al. (2008)
- V4.5_C1.1 – As above, modified to include atmospheric CO_2 content effects on transpiration and photosynthesis (Singels *et al.*, 2014)
- V4.5_C2.2 – The new model developed as a result of this study. It is intended that these model algorithms will be implemented in a forthcoming DSSAT CSM release.
- V4.5_C2.2_Rm0 – As above, modified such that maintenance respiration is not simulated. This version was used for testing only and will not be released.

A list of acronyms used in the model algorithm descriptions and equations is given in Section A6 of this appendix.

A2 Calculation of thermal time

Daily thermal time (TT, °C d) is calculated from daily mean temperature (T, °C) using three cardinal temperatures, namely: base temperature T_B (°C), below which process rates are zero; optimal temperature (T_O, °C), at which process rates are maximised; and upper temperature (T_U, °C), above which process rates are zero:

$$TT = \begin{cases} 0 \ for \ T \leq T_B \ or \ T \geq T_U & (1) \\ T - T_B \ for \ T_B < T \leq T_O & (2) \\ \left(1 - \frac{T - T_O}{T_U - T_O}\right) * (T_O - T_B) \ for \ T_O < T < T_U & (3) \end{cases}$$

Values for T_B, T_O and T_U for the different processes are given in Table A1. For photosynthesis a range of optimal temperatures between a lower and upper value ($T_{O,1}$ and $T_{O,2}$) were used. *TT* accumulation is illustrated in Figure A1.

Table A1. Cardinal temperatures for different processes. T_B, T_O and T_U refer to the base temperature, optimal temperature, and upper temperature, and values are based on references given below.

Process	T_B	T_O	T_U	References
Germination and shoot emergence	16	28	41	Liu *et al.* (1998); Smit (2010)
Leaf appearance rate	10	30	43	Inman-Bamber (1994); Campbell *et al.* (1998); Robertson *et al.* (1998); Sinclair *et al.* (2004); Singels *et al.* (2005); Bonnet *et al.* (2006);
Tiller emergence rate	16	35	48	Inman-Bamber (1994); Singels *et al.* (2005)
Leaf senescence rate	10	30	43	
Stalk elongation rate	16	35	48	Lingle and Smith (1991); Lingle (1999); Smit and Singels (2007)
Leaf elongation rate	10	30	43	
Root elongation rate	10	30	43	Sartoris (1929); Ryker and Edgerton (1931); Rands and Dopp (1938) (as quoted by van Dillewijn (1952)).
Photosynthesis[1]	10	20,40	47	Ebrahim *et al.* (1998)
Respiration[2]		40	47	Bieleski (1958) (as quoted by Liu and Bull (2001))

[1]The gross photosynthesis model has a T_O range, hence two values are specified.
[2]The maintenance respiration calculation does not make use of a T_B parameter.

Keating *et al.* (1999) used T_B, T_O and T_U of 9, 32 and 45 °C respectively for the calculation of thermal time, which apply to all processes in the APSIM-sugar model.

A3 Tillering

Tiller population in sugarcane increases with germination of underground buds into primary shoots, followed by the production of tillers from these; and decreases via tiller senescence to a relatively stable cultivar-specific final population of harvestable stalks, following canopy

closure. In terms of model formulation, primary shoots will be referred to as "primary tillers", and tillers will be referred to as "secondary tillers" for clarity and simplicity.

Tiller population (*TL*, tillers/m^2) is calculated differently for the tiller increase ('tillering') and senescence phases. For the tillering phase, *TL* is defined as the sum of primary (TL_P, tillers/m) and secondary tillers (TL_S, tillers/m), transformed to tillers per unit ground area using row-spacing (*RSP*, m):

$$TL = (TL_P + TL_S) * \frac{1}{RSP} \quad (4)$$

TL_P is calculated after a thermal time period for germination has elapsed since crop start, defined as the date of emergence of the first primary tiller (genetic trait parameters *TTPLTNEM* and *TTRATNEM*, for plant and ratoon crops respectively). TL_P on day d (i.e. $TL_{P,d}$) is calculated as:

$$TL_{P,d} = \left(\Delta TL_{P0,d} * SWDF_{30}\right) + TL_{P,d-1} \quad (5)$$

where $\Delta TL_{P0,d}$ is the daily change in the potential (i.e. in the absence of water stress) number of primary tillers (TL_{P0}, tillers/linear m) appearing on subsequent days, limited by a water stress factor ($SWDF_{30}$, described by Singels *et al.* (2008)), and $TL_{P,d-1}$ is the previous day's primary tiller population. $\Delta TL_{P0,d}$ on day *d* is calculated as follows:

$$\Delta TL_{P0,d} = TL_{P0,d} - TL_{P0,d-1} \quad (6)$$

where

$$TL_{P0,d} = B * (1 - e^{f_{TL} * TT_{EM,d}}) \quad for\ 0 \leq TT_{EM} \leq 600 \quad (7)$$

where $TT_{EM,d}$ is the thermal time (°C d) accumulated from emergence on day *d*, calculated according to Table A1, f_{TL} is an empirical parameter, the value of which was determined using data from Smit (2010) (f_{TL} = -0.00707), and *B* is the specified number of viable buds (/m) in the soil at crop start.

Whenever one or more whole new primary or secondary tillers appears per 1 m of row (i.e. 10 000 tillers/ha when row-spacing is 1.0 m), a new tiller cohort is created. Timing for appearance of secondary tillers is calculated independently per cohort of primary tillers. The implementation of this algorithm requires that TL_P is a whole (integer) number each day of the simulation. In cases where the daily change in TL_P is not a whole (integer) number, the fractional remainder is accumulated and added to the daily change the following day.

The total number of secondary tillers TL_S (tillers/m) is calculated as the sum of secondary tillers on day *d*-1 and the sum of new secondary tillers that develop on day *d*, i.e.:

$$TL_{S,d} = \sum_{n=1}^{N} \Delta TL_{S,n} + TL_{S,d-1} \tag{8}$$

for *N* primary tiller cohorts, where *n* refers to each individual primary tiller cohort.

Tillering rate (ΔTL_S, secondary tillers/cohort/d), is calculated per primary tiller cohort *n* and decreases linearly with increased mutual shading from other tillers:

$$\Delta TL_{S,n} = \Delta TT_T * TAR_O * \left(1 - \frac{FiPAR}{FiPAR_C}\right) * SWDF_{30} * TL_{P,n} \tag{9}$$

where ΔTT_T is the daily thermal time accumulation driving tiller development (calculated using Equation (1) and cardinal temperature values described in Table A1), TAR_O is a cultivar parameter defined as the maximum rate of secondary tiller appearance per primary tiller (tillers/tiller/°C d) under ideal environmental conditions, *FiPAR* represents fractional interception of photosynthetically-active radiation, $FiPAR_C$ is the *FiPAR* above which tillering ceases (value of 0.75 derived from data presented by Jones *et al.*, 2011, and supported by data from Inman-Bamber, 1994 and Zhou *et al.*, 2003), and $TL_{P,n}$ is the number of primary tillers in primary tiller cohort *n* (all values calculated on day *d*).

The calculation of tiller senescence was not changed.

A4 Photosynthesis, respiration and biomass accumulation

Daily biomass accumulation (*⊿TDM*, t/ha/d) is calculated as the difference between gross photosynthesis (P_G, t/ha/d) and the sum of growth (R_g, t/ha/d) and maintenance (R_m, t/ha/d) respiration:

$$\Delta TDM = P_G - R_g - R_m \tag{10}$$

P_G is calculated as:

$$P_G = PARCE * FiPAR * PAR * \frac{1}{100} \tag{11}$$

where *PAR* (MJ/m^2/d) is daily photosynthetically-active incident solar radiation, and *PARCE* (g/MJ) is the rate of photosynthesis per unit of intercepted *PAR*.

PARCE is calculated as a function of crop water status ($SWSI_{PT}$), effective temperature (F_T), an atmospheric CO_2 concentration ([CO2], ppm) factor (F_{CO2}), and a maximum rate of photosynthesis per unit of intercepted *PAR* (cultivar parameter *MaxPARCE*, g/MJ):

$$PARCE = MaxPARCE * F_T * SWSI_{PT} * F_{CO2} \tag{12}$$

$$F_T = \begin{cases} 1 \ for \ T_{O,1} \geq T \geq T_{O,2} & (13) \\ \max\left(0, 1 - \frac{(T - T_{O,2})}{T_U - T_{O,2}}\right) \ for \ T > T_{O,2} & (14) \\ 1 - \frac{(T_{O,1} - T)}{T_{O,1} - T_B} \ for \ T < T_{O,1} & (15) \end{cases}$$

where $T_{O,1}$ and $T_{O,2}$ are the lower and upper values of the optimal temperature range (values specified in Table A1). The value of *MaxPARCE* was determined by trial and error to minimise differences between simulated and observed aerial dry biomass for a calibration dataset for the South African reference cultivar NCo376. Temperature effects on photosynthesis are illustrated in Figure A1. The calculation of $SWSI_{PT}$ is explained in Section A4.1.

The direct fertilisation effect of elevated [CO2] on gross photosynthesis is captured with a relative photosynthesis rate multiplier F_{CO2} (Equation (12)). The value of F_{CO2} is determined by a lookup function, which interpolates linearly between cardinal points in a set defining the relationship between F_{CO2} and [CO2] (Table A2). The set of parameter values is defined in the DSSAT species file, allowing modification without recompiling the source code.

Most recent research found little evidence of a direct photosynthesis enhancement response to elevated [CO2], so the cardinal points currently in use do not exceed an F_{CO2} value of 1.0. As pointed out by Jones *et al.* (2015) some workers (Vu *et al.* (2006), de Souza *et al.* (2008) and Allen *et al.* (2011)) reported increased photosynthesis rates at elevated [CO2] in pot experiments, but improved crop water status through stomatal response may have contributed significantly to these observed responses. Webster *et al*. (2009) assumed an increase in radiation use efficiency of 1.43% per 100 ppm increase in [CO2] for a climate change impact study with APSIM-Sugar, while Biggs *et al*. (2013) also used this value in their climate change study. Stokes *et al.* (2016) found no significant effect on photosynthesis when crop water status was optimal, while Malan *et al.* (2017) found no significant effects on biomass production in the absence of water stress.

The values of F_{CO2} at [CO2] values lower than 330 ppm are based on work by Ward *et al*. (1999) and Pinto *et al*. (2014) which suggest that F_{CO2} for crops with the C4 photosynthesis pathways only starts declining when [CO2] drops below about 270 ppm. A linear decline is assumed between [CO2] values of 180 and 15 (assumed CO_2 compensation point). The inclusion of the functionality in the model is primarily to make provision for a direct [CO2] response, particularly under elevated [CO2] conditions, if/when new research points provides conclusive evidence and descriptions thereof.

Table A2. Cardinal points defining the lookup function of F_{CO2} *(gross photosynthesis rate multiplier, Eq. (12)) vs atmospheric* CO_2 *concentration ([CO2] in ppm).*

[CO2]	15	180	270	330	400	490	570	750	990	1500
F_{CO2}	0.00	0.75	1.00	1.00	1.00	1.00	1.00	1.00	1.00	1.00

R_g is calculated as a function of daily structural growth rate, rather than daily P_G (Liu and Bull, 2001; Amthor, 2000). In the model, fibre growth is approximated by deducting the previous day's daily sucrose accumulation ($\Delta SUCM_{d-1}$, t/ha/d) from ΔTDM:

$$R_g = RESP_{CF} * (\Delta TDM - \Delta SUCM_{d-1}) \quad (16)$$

where $RESP_{CF}$ (0.33 g/g) is the fraction of gross photosynthesis lost through respiration associated with fibre synthesis. Values for $RESP_{CF}$ in the literature range from 0.19 (Amthor, 2000) to 0.33 (Thornley and Johnson, 1990 (as quoted by Liu and Bull, 2001)).

R_m is only calculated for the maintenance of green, living tissue (green leaf, meristem and roots) and for the pool of stored sucrose (van der Merwe and Botha, 2014), as opposed to respiration to maintain the total dry biomass (*TDM*, t/ha) of plant including dead material and old stalk fibre. The fibre and sucrose pools each have unique energy requirements in terms of the fraction of biomass lost through respiration ($RESP_{CON}$), and the fraction also depends on temperature. R_m for biomass pool p is calculated as:

$$R_{m,p} = \begin{cases} DM_p * RESP_{CON,p} * RESP_{Q10}^{\left(\frac{T-10}{10}\right)} \; for \; T \leq T_O & (17) \\ DM_p * RESP_{CON,p} * RESP_{Q10}^{\left(\frac{T_O-10}{10}\right)*\left(1-\frac{T-T_O}{T_U-T_O}\right)} \; for \; T > T_O & (18) \end{cases}$$

where DM_p represents the dry mass (t/ha) of biomass pool p.

The values derived for $RESP_{CON,p}$ for V4.5_C2.2 were 0.00292 g/g/d for green leaf and roots, and 0.00121 g/g/d for stalk sucrose. These values were chosen so that (1) a whole crop daily *Rm*/*TDM* of approximately 0.003 g/g (Inman-Bamber and Thompson, 1989) was achieved at a temperature of 25 °C (based on a preliminary simulation of a typical hypothetical crop) and (2)

the ratio between the respiration coefficients for sucrose and structural growth equalled 0.416:1 (following Liu and Bull, 2001). Parameter $RESP_{Q10}$ determined the steepness of the exponential increase with temperature and had a value of 1.68 (derived from Liu and Bull, 2001). Respiration rates following the new (Equation (17)) and original approaches are illustrated in Figure A2.

It should be noted that Gifford (2003) concluded from his review that assuming a conservative ratio between total respiration and photosynthesis would be an effective and practical way of simulating respiration rate in crop models. This effectively eliminates the need for simulating maintenance respiration. Everingham *et al*. (2015) also used a zero-maintenance respiration option in some of their simulations to project likely impacts of climate change on sugarcane yields in Australia. For this reason, the V4.5_C2.2_Rm0 version of the model was developed and evaluated. Values for $RESP_{CON,p}$ were set to 0.0 for V4.5_C2.2_Rm0, in order to disable calculation of R_m; *MaxPARCE* was also recalibrated to compensate for this change.

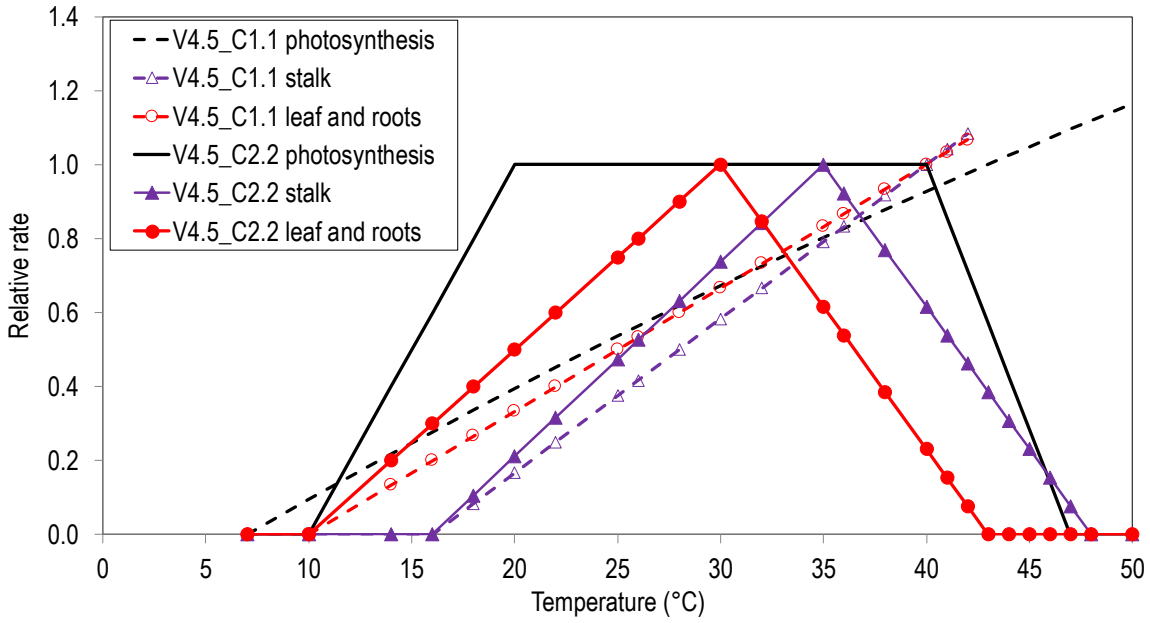

Figure A1. Functions illustrating the relationship between the relative rate of processes (photosynthesis, stalk elongation, leaf appearance and elongation, and root elongation) and daily mean temperature. Solid lines show functions in the V4.5_C2.2 and V4.5_C2.2_Rm0 versions of the DSSAT-Canegro model, while dashed line show functions in V4.5_C1.1.

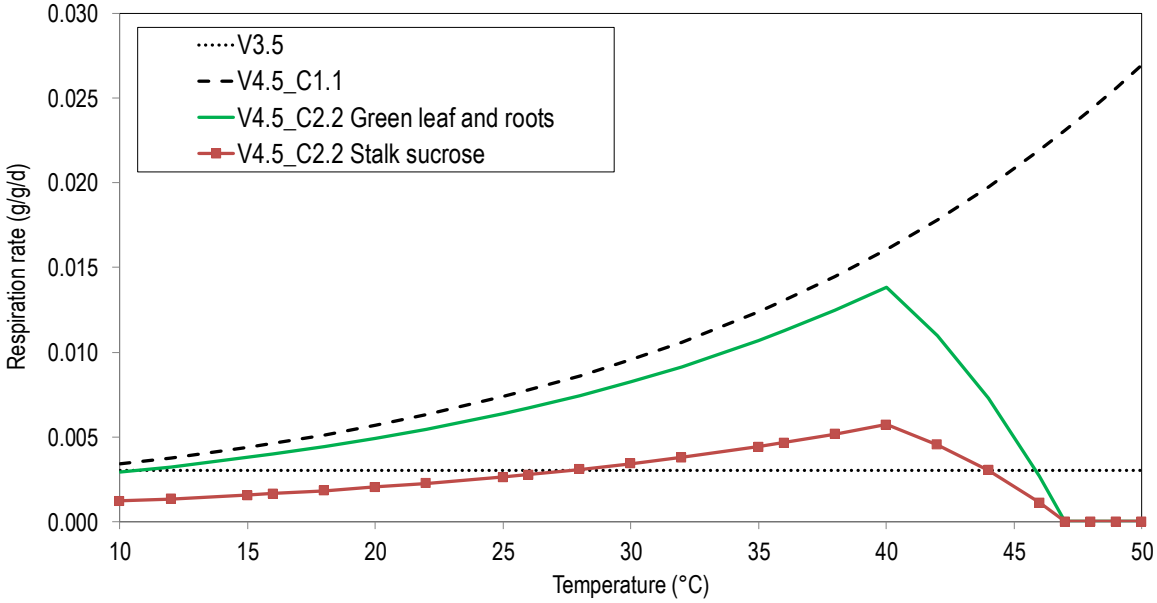

Figure A2. Simulated relationship between rate of maintenance respiration and daily mean temperature, expressed as daily mass respired per unit mass of the relevant plant component. Older versions of DSSAT-Canegro (V3.5 (Cheeroo-Nayamuth et al., 2003) and V4.5_C1.1) related respiration to total (live and dead biomass), while in version V4.5_C2.2 respiration is only considered for live leaves, roots and meristem mass, and for sucrose stored in the stalk.

A5 Supply-limited water uptake

A5.1 Water deficit stress

Singels *et al.* (2010) showed that the CERES-based (Jones and Kiniry, 1986) Canegro model simulation of reduced water uptake (and reduced photosynthesis) during water stress events was much more abrupt than what was observed, and that simple models based on soil water content thresholds simulated a more gradual decline that mimicked observations more closely. It was decided to adopt the AquaCrop (Steduto *et al.*, 2009) approach of using process-specific soil water depletion thresholds that depend on atmospheric evaporative demand to simulate the impacts (the 'soil water satisfaction index', *SWSI*) of water supply and demand dynamics on transpiration and photosynthesis ($SWSI_{PT}$) and expansive growth ($SWSI_G$).

The calculation of $SWSI_X$ for the soil profile, when soil water content is below field capacity (FC), considers root length density (RLV_i, cm/cm^3) and soil layer thickness (Z_i, cm) per soil layer i, in addition to per-layer soil water factor values ($F_{W,i}$) specific to each process X (photosynthesis and transpiration, or expansive growth).

$$SWSI_X = \frac{\sum_{i=1}^{NLYR}\left(F_{W,X,i} * RLV_i * Z_i\right)}{\sum_{i=1}^{NLYR}(RLV_i * Z_i)} \tag{19}$$

for $NLYR$ soil layers, and where

$$F_{W,X,i} = 1 - \frac{e^{(DREL_{X,i} * f_{FW})} - 1}{e^{f_{FW}} - 1} \quad for \;\; SWC_i \geq FC_i \tag{20}$$

where

$$DREL_{X,i} = \begin{cases} \dfrac{RSWD_i - PUP}{PLO_X - PUP} & for \;\; PLO_X > PUP \\ 0 & for \;\; PLO_X \leq PUP \end{cases} \tag{21}$$

where $DREL_i$ is limited to values in the range 0.0-1.0, and $RSWD$ is the relative soil water depletion, calculated as:

$$RSWD_i = 1 - \frac{SWC_i - WP_i}{FC_i - WP_i} \tag{22}$$

where SWC is soil water content (cm^3/cm^3), FC_i is field capacity (cm^3/cm^3) and WP_i (cm^3/cm^3) is the permanent wilting point for soil layer i. Parameter f_{FW} (numerical value of 2.0 assumed) in Equation (20) determines the shape of the curve describing the relationship between $F_{W,i}$ and $DREL_i$.

A diminishing rate of decline in soil water thresholds with increasing atmospheric evaporative demand (represented by reference sugarcane evaporation, $E_{O,cane}$, calculated as the product of FAO56 short grass reference evaporation following Allen *et al.* (1998) and the sugarcane crop evaporation coefficient $EORATIO$ = 1.15 following Singels *et al.*, 2008) was considered more

appropriate than the almost linear decline used in the AquaCrop approach (Raes *et al*., 2009). Similar relationships between soil water content threshold levels and evaporative demand were also used by Slabbers (1979), Doorenbos and Kassam (1979) and in the Wofost model (Supit *et al.*, 1994). Hence, the upper (*PUP*) and lower (*PLO*) fractional depletion thresholds where a reduction in process rates starts, and where the process rate declines to zero, were calculated as:

$$PUP = \frac{E_{0PUP}}{E_{O,cane} + E_{0PUP}} \quad (23)$$

$$E_{0PUP} = 0.4186 * e^{(4.8622 * PUP_5)} \quad (24)$$

$$PLO_X = PUP_{5,X} + O_X \quad (25)$$

where $PUP_{5,X}$ is the upper depletion threshold at the reference $E_{O,cane}$ of 5 mm/d, PLO_X is the lower depletion threshold at the same reference $E_{O,cane}$, and O_X is a relative soil water depletion offset, specific to process *X;* O_{PT} = 0.35 (photosynthesis and transpiration) and O_G = 0.50 (expansive growth). Equation (23) represents the diminishing rate of decline in *PUP* with increasing $E_{O,cane}$, while Equation (24) was parameterised to produce values that closely match those produced by the method of Slabbers (1979). Equations (23) and (24) also produce *PUP* values close to those produced by the AquaCrop method (Raes *et al.*, 2009) for a relatively wide range of $E_{O,cane}$ values (3-12 mm/d). Outside this range (below 3 and above 12 mm/d), the values produced by Equations (23) and (24) are higher than those produced by the AquaCrop method.

PUP_5 for photosynthesis and transpiration ($PUP_{5,PT}$) is a cultivar-specific parameter that typically varies from 0.40 to 0.65, depending on the sensitivity to drought stress (low values indicate high sensitivity – i.e. early stomatal closure). A value of 0.60 was assumed for NCo376 based on water uptake and photosynthesis data from Singels *et al.* (2010), which was derived from data collected in experiments described by Singels *et al.* (2000) and Smit and Singels (2006), and by comparing $SWSI_{PT}$ simulated by the two model versions for these experiments.

Per-layer $F_{W,i}$ values for the calculation of *SWSI* for photosynthesis and transpiration ($SWSI_{PT}$) are denoted $F_{W,PT,i,}$. PUP_5 for expansive growth ($PUP_{5,G}$) is considered a species parameter with value of 0.20, indicating the extreme sensitivity of expansive growth to water stress (Singels *et al.*, 2000; Smit and Singels, 2006; Rossler, 2014).

The relationships between *SWSI* and soil water depletion are illustrated in Figure A3.

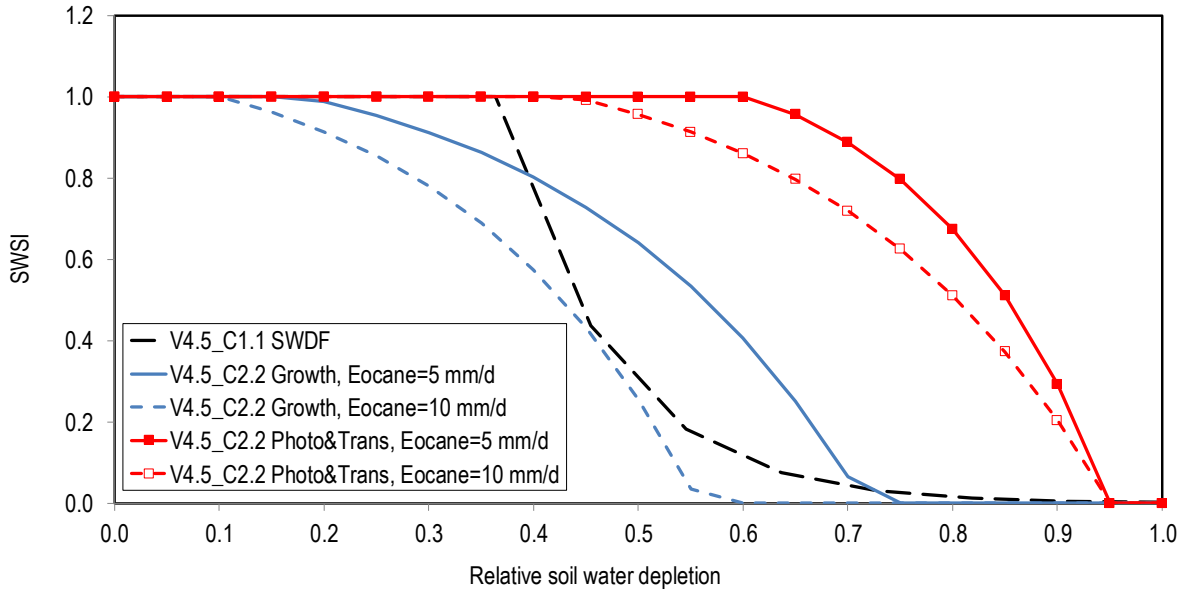

Figure A3. The AquaCrop soil water satisfaction index (SWSI) as implemented in DSSAT-Canegro versions V4.5_C2.2 and V4.5_C2.2_Rm0, as a function of relative soil water depletion and atmospheric evaporative demand ('Eocane'), compared to the soil water deficit factors calculated in V4.5_C1.1. The graphs show that photosynthesis and transpiration are less sensitive to soil water deficit than expansive growth.

A5.2 Aeration stress

Aeration stress is created by a lack of oxygen in the root system caused by waterlogged conditions.

In the V4.5_C1.1 model, reductions in transpiration due to waterlogging are calculated in a common module as part of the DSSAT CSM water uptake routine. The parameter *PORMIN* (cm^3/cm^3) specifies a volumetric pore-space threshold, at a soil water content above which

aeration stress starts to reduce potential root water uptake by a factor proportional to the pore space occupied by excess soil moisture. At least two days of consecutive waterlogged conditions are required before stress impacts are calculated. During the implementation of the revised aeration stress calculation in V4.5_C2.2, it was discovered that *PORMIN* had been inadvertently initialised to 0 cm^3/cm^3 in the Canegro plant module, with the result that no aeration stress is ever actually calculated in V4.5_C1.1.

In the revised V4.5_C2.2 model, the soil profile water satisfaction index, *SWSI*, is in this case calculated as a function of the extent to which soil water content (*SWC*) exceeds field capacity (*FC*). *SWSI* is assigned the $F_{W,i}$ value of the layer with the highest (least limiting) $F_{W,i}$ value.

$$SWSI = \max(F_{W,i}) \tag{26}$$

$$F_{W,i} = \frac{SWC_i - FC_i}{SWC_i - SAT_i} \quad for\ SWC_i > FC_i \tag{27}$$

where SAT_i is soil water content at saturation for layer i. This recognizes the fact that if any part of the root system can access air, this will be sufficient for the whole system.

These changes make this version of the model far more sensitive to the difference between *FC* and *SAT* than previous model versions.

A5.3 Impact of water stress on plant processes

The impact of soil water availability on gross photosynthesis rate (P_G) is captured with the soil water satisfaction index ($SWSI_{PT}$, described in Equation (12)). Soil water availability also affects structural growth rates by limiting leaf elongation rate (*LER*, cm/d) and stalk elongation rate (*SER*, cm/d), as well as rooting depth penetration rate (*RER*, mm/d); the potential rates for these processes (the products of LER_O, SER_O and RER_O (referring to leaves, stalks and rooting front elongation respectively) and their corresponding daily thermal time accumulation amounts (ΔTT_{LE}, ΔTT_{SE}, ΔTT_{RE})) are reduced by $SWSI_G$. These can be described conceptually as follows:

$$LER = LER_O * \Delta TT_{LE} * SWSI_G \quad (28)$$

$$SER = SER_O * \Delta TT_{SE} * SWSI_G \quad (29)$$

$$RER = RER_O * \Delta TT_{RE} * SWSI_G \quad (30)$$

The soil water availability effect on daily transpiration rate (*TRANS*, mm/d) is calculated as the sum of water uptake from individual soil layers (RWU_i, cm/d):

$$TRANS = \sum_{i=1}^{NLYR} RWU_i * 10.0 \quad (31)$$

where RWU_i is calculated by apportioning $F_{W,PT,i}$, according to Z_i and RLV_i:

$$RWU_i = \frac{F_{W,PT,i} * RLV_i * Z_i}{\sum_{i=1}^{NLYR}(RLV_i * Z_i)} * TRANS_O \quad (32)$$

where $TRANS_O$ is potential transpiration (mm/d).

A5.4 Effect of atmospheric carbon dioxide content on transpiration

It was decided to keep the DSSAT algorithm for simulating [CO2] effect on transpiration, that was part of V4.5_C1.1 (described by Boote *et al.* 2010), unchanged in the new model (V4.5_C2.2). It is nevertheless described here to avoid any confusion and for the record.

Potential transpiration rate $TRANS_O$ (mm/d) is calculated in the DSSAT CSM as

$$TRANS_O = E_{O,cane} * FiPAR * TRATIO \quad (33)$$

and

$$E_{O,cane} = E_O * EORATIO \quad (34)$$

where $E_{O,cane}$ is sugarcane reference evaporation calculated as the product of a short grass reference evaporation rate (E_O, mm/d) and a crop evaporation multiplier (*EORATIO*, set to 1.15 for sugarcane (Singels *et al.*, 2008)). E_O is calculated using the FAO-56 (Penman-Monteith, Allen *et al.*, 1998) short grass reference evaporation algorithm. The effect of [CO2] on daily transpiration rate is captured by a multiplier variable (*TRATIO*) representing the effect of CO_2

on stomatal resistance to gaseous exchange and defined as the ratio of potential transpiration rate at a given [CO2] to that at a reference [CO2] of 330 ppm.

This functionality is part of the DSSAT Cropping System Model (Jones *et al.*, 2003). *TRATIO* is calculated in DSSAT CSM as:

$$TRATIO = \frac{\Delta + \gamma * \left(1.0 + \frac{RC_{330}}{RA}\right)}{\Delta + \gamma * \left(1.0 + \frac{RC}{RA}\right)} \quad (35)$$

where Δ is the slope of the saturated vapour pressure vs temperature curve, γ is the psychrometric constant, RC_{330} (s/m) is canopy resistance for gaseous exchange at [CO2] of 330 ppm, *RC* (s/m) is canopy resistance at a given [CO2], and *RA* (s/m) is boundary layer resistance. Canopy resistance *RC* is calculated from stomatal resistance *RS* (s/m) and a reference leaf area index (LAI_{ref} = 2.88 m^2/m^2) while *RS* is calculated from [CO2] and an assumed leaf boundary resistance (*RB*) of 10 s/m, following Allen *et al.* (1985):

$$RC = \frac{RS}{\left(0.5 * LAI_{ref}\right)} \quad (36)$$

$$RS = \left(\frac{1.0}{0.0328 - 5.49x10^{-5} * [CO2] + 2.96x10^{-8} * [CO2]^2}\right) + RB \quad (37)$$

In the climate change study by Everingham *et al*. (2015), a similar approach was used to account for the [CO2] effect on sugarcane transpiration. Transpiration was calculated with the Penman-Monteith equation. *RC* was calculated from *RS* using LAI_{ref} of 3.5 (Equation (36)). *RS* was calculated as linear function of [CO2], increasing by 12 s/m for every 100-ppm increase in [CO2] from the reference value of 100 s/m at [CO2] = 325 ppm. This method was also proposed by Stokes *et al*. (2016). The DSSAT algorithm yields stomatal resistance values that are lower than those calculated by the method of Everingham *et al*. (2015) (e.g. 135 vs 151 s/m at [CO2] of 750 ppm) and the rate of *RS* increase per unit increase in [CO2] varies from 12 to 17 s/m per 100 ppm increase in [CO2].

A6 List of acronyms

Table A3 lists the acronyms used in the model description.

Table A3. Acronym descriptions. Full definitions can be found in the text.

Variable name / abbreviation	Description and units
[CO2]	Atmospheric CO_2 concentration (ppm)
ADM	Aerial dry biomass (t/ha)
ADM_H	Aerial dry biomass at harvest (t/ha)
APE	Average prediction error
B	Number of viable buds in the soil at crop start
D	Current day of simulation
DM_p	Dry mass of biomass pool *p*
$DREL_i$	Relative soil water depletion below the upper threshold for soil layer *i*
$DREL_{X,i}$	*DREL* specific to process *X* for soil layer *i*
E_O	FAO-56 short grass reference evaporation rate (mm/d)
$E_{O,cane}$	Sugarcane reference evaporation rate (mm/d)
E_{OPUP}	The $E_{O,cane}$ value where PUP equals a value of 0.5
EORATIO	Sugarcane crop evaporation coefficient
ET	Evapotranspiration (mm)
FC	Soil water content at field capacity (cm^3/cm^3)
FC_i	Soil water content at field capacity of soil layer *i* (cm^3/cm^3)
F_{CO2}	Atmospheric CO_2 concentration factor for controlling photosynthesis rate
f_{FW}	Shape factor for the relationship between the soil water satisfaction index and relative soil water depletion
FiPAR	Fractional interception of photosynthetically active radiation
$FiPAR_C$	FiPAR level at which tillering ceases due to light competition effects
F_T	Temperature factor for controlling photosynthesis rate
f_{TL}	Exponential shape factor for the relationship between tiller appearance rate and thermal time
$F_{W,i}$	Soil water status factor per soil layer *i*
$F_{W,PT,i}$	
$F_{W,X,i}$	Soil water status factor for process X per layer *i*
i	Soil layer identifier
IRR	Irrigation demand (mm)
LAI	Leaf area index (m^2/m^2)
LAI_{ref}	Reference leaf area index (m^2/m^2)
LER	Leaf elongation rate (cm/d)
LER_O	Potential leaf elongation rate (cm/d/°C d)
MaxPARCE	Maximum conversion efficiency of intercepted photosynthetically active radiation to gross photosynthate (g/MJ)
N	Total number of primary tiller cohorts
n	Primary tiller cohort identifier
NLYR	Number of soil layers

Variable name / abbreviation	Description and units
O_G	Soil water depletion offset for expansive growth
O_{PT}	Soil water depletion offset for photosynthesis and transpiration
O_X	Soil water depletion offset for process *X*
p	Biomass pool identifier
PAR	Daily incident photosynthetically active radiation (MJ/m^2)
PARCE	Conversion efficiency of intercepted photosynthetically active radiation to gross photosynthate (g/MJ)
PAWC	Plant available soil water-holding capacity (cm^3/cm^3)
P_G	Gross photosynthesis rate (t/ha/d)
PLO_X	Lower fractional soil water depletion threshold (cm^3/cm^3) for process *X*
PUP	Upper fractional soil water depletion threshold (cm^3/cm^3)
PUP_5	Upper soil water depletion threshold at reference conditions (cm^3/cm^3)
$PUP_{5,G}$	Upper soil water depletion threshold at reference conditions (cm^3/cm^3) for expansive growth
$PUP_{5,PT}$	Upper soil water depletion threshold at reference conditions (cm^3/cm^3) for process photosynthesis and transpiration
$PUP_{5,X}$	Upper soil water depletion threshold under reference conditions (cm^3/cm^3) for process *X*
RA	Boundary layer resistance to gaseous exchange (s/m)
RB	Leaf boundary resistance to gaseous exchange (s/m)
RC	Canopy resistance to gaseous exchange (s/m)
RC_{330}	Canopy resistance to gaseous exchange at 330 ppm atmospheric CO_2 content (s/m)
RER	Daily change in rooting front depth (mm/d)
RER_O	Potential daily change in rooting front depth (mm/d/°C d)
$RESP_{CF}$	Fraction of gross photosynthate lost through respiration associated with fibre synthesis
$RESP_{CON,p}$	Maintenance respiration coefficient for biomass pool *p*
$RESP_{Q10}$	Temperature sensitivity factor for maintenance respiration rate
R_g	Growth respiration rate (t/ha/d)
RGP	Reduced growth phenomenon
RLV_i	Root length density of soil layer *i* (cm/cm^3)
R_m	Maintenance respiration rate (t/ha/d)
$R_{m,p}$	Maintenance respiration rate (t/ha/d) for biomass pool *p*
RMSE	Root mean squared error
RMSE%	RMSE expressed as a percentage of the average observed value
RS	Stomatal resistance to gaseous exchange (s/m)
RSP	Row-spacing (m)
$RSWD_i$	Relative soil water depletion for soil layer *i* (cm^3/cm^3)
RUE_A	Apparent radiation use efficiency (g/MJ)
RWU_i	Root water uptake from soil layer *i* (mm/d)
SAT	Soil water content at saturation (cm^3/cm^3)
SAT_i	Soil water content at saturation for soil layer *i* (cm^3/cm^3)
SDM	Stalk dry mass (t/ha)
SDM_H	Stalk dry mass at harvest (t/ha)
SER	Stalk elongation rate (cm/d)

Variable name / abbreviation	Description and units
SER_O	Potential stalk elongation rate (cm/d/°C d)
SUCM	Stalk sucrose mass (t/ha)
SWC_i	Soil water content of soil layer *i* (cm^3/cm^3)
$SWDF_{30}$	Soil water deficit factor affecting tillering rate
SWSI	Soil water satisfaction index
$SWSI_G$	Soil water satisfaction index affecting expansive growth
$SWSI_{PT}$	Soil water satisfaction index affecting photosynthesis and transpiration
$SWSI_X$	Soil water satisfaction index affecting process *X*
T	Mean daily air temperature (°C)
TAR_O	Maximum secondary tiller appearance rate per primary tiller per unit thermal time (tillers/tiller/ (°C d))
T_B	Base temperature (°C)
TDM	Crop total dry biomass (t/ha)
TE_A	Apparent transpiration efficiency (g/kg)
TL	Tiller population (tillers/m^2)
TL_P, $TL_{P,d}$	Primary tiller population (tillers/m) on day *d*
$TL_{P,d-1}$	Previous day's primary tiller population (tillers/m)
$TL_{P,n}$	Primary tiller population of tiller cohort *n*
TL_{P0}, $TL_{P0,d}$	Potential primary tiller population (tillers/m/d) on day *d*
TL_S, $TL_{S,d}$	Secondary tiller population (tillers/m) on day *d*
$TL_{S,d-1}$	Previous day's secondary tiller population (tillers/m)
T_O	Optimal daily mean temperature (°C)
$T_{O,1}$	Lower bound of optimal temperature range for photosynthesis (°C)
$T_{O,2}$	Upper bound of optimal temperature range for photosynthesis (°C)
TRANS	Transpiration rate (mm/d)
$TRANS_O$	Potential transpiration rate (mm/d)
TRATIO	Potential transpiration rate under a given atmospheric CO_2 concentration relative to the rate at CO_2 concentration of 330 ppm
TT	Accumulated thermal time (°C d)
TT_{EM}, $TT_{EM,d}$	Accumulated thermal time affecting shoot emergence (°C d) on day *d*
T_U	Upper temperature threshold (°C)
WP_i	Soil water content at wilting point for soil layer *i* (cm^3/cm^3)
X	Physiological process identifier
Z_i	Thickness of soil layer *i* (cm)
γ	Psychrometric constant (kPa/°C)
Δ	Slope of the saturated vapour pressure vs temperature curve (kPa/°C)
$\Delta SUCM_{d-1}$	Previous day's change in sucrose mass (t/ha/d)
ΔTDM	Daily change in total dry biomass (t/ha/d)
$\Delta TL_{P0,d}$	Daily change in potential primary tiller population (tillers/m/d) on day *d*
ΔTL_S	Daily change in secondary tiller population(tillers/m)
$\Delta TL_{S,n}$	Daily change in the number of secondary tillers (tillers/m) for primary tiller cohort *n*
ΔTT_{LE}	Daily thermal time calculated using cardinal temperatures for leaf elongation (°C d)

Variable name / abbreviation	Description and units
ΔTT_{RE}	Daily thermal time calculated using cardinal temperatures for root elongation (°C d)
ΔTT_{SE}	Daily thermal time calculated using cardinal temperatures for stalk elongation (°C d)
ΔTT_{T}	Daily thermal time calculated using cardinal temperatures for tillering (°C d)

A7 References

Allen, L.H., Jones, P. and Jones, J.W. 1985. Rising atmospheric CO_2 and evapotranspiration. In: Proceedings of the National Conference on Advances in Evapotranspiration held in Chicago, Illinois from 16-17 December 1985. ASAE publication, St Joseph, Michigan, pp. 13-27.

Allen, L.H. Jr., Vu, J.C.V., Anderson, J.C. and Ray, J.D. 2011. Impact of elevated carbon dioxide and temperature on growth and sugar yield of the C4 sugarcane. Current Topics in Plant Biology 11: 171-178.

Allen, R.G., Pereira, L.S., Raes, D. and Smith, M. 1998. Crop evapotranspiration: guidelines for computing crop water requirements. In: FAO Irrigation and Drainage Paper 56. Food and Agriculture Organisation of the United Nations, Rome, Italy.

Amthor, J.S. 2000. The McCree-Penning De Vries–Thornley paradigms: 30 years later. Annals of Botany 86: 1-20.

Bieleski, R.L. 1958. The physiology of sugarcane. II. The respiration of harvested sugarcane. Aust. J. Biol. Sci. 11: 315–328.

Biggs, J.S., Thorburn, P.J., Crimp, S., Masters, B. and Attard, S.J. 2013. Interactions between climate change and sugarcane management systems for improving water quality leaving farms in the Mackay Whitsunday region. Aust. Agric. Ecosyst. Environ. 180, 79–89.

Bonnet, G., Hewitt, M.L. and Glassop, D. 2006. Effect of high temperature on the growth and composition of sugarcane internodes. Aust. J Agric. Res. 57:1087-1095.

Boote, K.J., Allen, L.H. Jr., Prasad, P.V.V. and Jones, J.W. 2010. Testing effects of climate change in crop models. In: Hillel, D. and Rosenzweig. C. (eds). Handbook of climate change and agro-ecosystems: Impacts, adaptation, and mitigation., ICP series on climate change impacts, adaptation, and mitigation Vol. 1. Imperial College Press pp. 109–129.

Campbell, J.A., Robertson, M.J. and Grof, C.P.L. 1998. Temperature effects on node appearance in sugarcane. Australian Journal of Plant Physiology 25: 815-818.

Cheeroo-Nayamuth, F.B., Bezuidenhout, C.N., Kiker, G.A. and Nayamuth, A.R.H. 2003. Validation of Canegro-DSSAT V3.5 for contrasting sugarcane varieties in Mauritius. Proceedings of the Annual Congress - South African Sugar Technologists' Association 77:601-604.

De Souza, A.P., Gaspar, M., da Silva, E.A., Ulian, E.C., Waclawovsky, A.J., Nishiyama M.Y.Jr., dos Santos, R.V., Teixeira, M.M., Souza, G.M., Buckeridge, M.S. 2008. Elevated CO2 increases photosynthesis, biomass and productivity, and modifies gene expression in sugarcane. Plant, Cell and Environment 31: 1116-1127.

Doorenbos, J. and Kassam, A.H. 1979. Yield Response to Water. Food and Agriculture Organization of the United Nations, Rome, FAO Irrigation and Drainage Paper 33, p. 193.

Ebrahim, M.K., Vogg, G., Osman, M.N.E.H. and Komor, E. 1998. Photosynthetic performance and adaptation of sugarcane at suboptimal temperatures. J Plant Physiology: 153: 587-592.

Everingham, Y., Inman-Bamber, N.G., Sexton, J. and Stokes, C. 2015. A dual ensemble agroclimate modelling procedure to assess climate change impacts on sugarcane production in Australia. Agricultural Sciences 6: 870-888.

Gifford, R.M. 2003. Plant respiration in productivity models: conceptualization, representation and issues for global terrestrial carbon-cycle research. Functional Plant Biology 30:171-186.

Inman-Bamber, N.G. 1994. Temperature and seasonal effects on canopy development and light interception of sugarcane. Field Crops Research 36:41-51.

Inman-Bamber, N.G. and Thompson, G.D. 1989. Models of dry matter accumulation by sugarcane. Proc. S. Afr. Sug. Technol. Ass. 63: 212-216.

Jones, C.A. and Kiniry, J.R. 1986. CERES-Maize Model: A Simulation Model of Maize Growth and Development. Texas A&M University Press, p. 194.

Jones, J.W., Hoogenboom, G., Porter, C.H., Boote, K.J., Batchelor, W.D., Hunt, L.A., Wilkens, P.W., Singh, U., Gijsman, A.J. and Ritchie, J.T. 2003. The DSSAT cropping system model. European Journal of Agronomy 18:235-265.

Jones, M.R., Singels, A., and Inman-Bamber, N.G. 2011. Simulating source and sink control of structural growth and development and sucrose accumulation in sugarcane. Proc. S. Afr. Sug. Technol. Ass. 84: 157 – 163.

Jones, M.R., Singels, A. and Ruane, A. 2015. Simulated impacts of climate change on water use and yield of irrigated sugarcane in South Africa. Agric. Systems 139: 260–270.

Keating, B.A., Robertson, M.J. and Muchow, R.C. 1999. Modeling sugarcane production systems I. Development and performance of the sugarcane module. Field Crops Research 61: 253-271.

Lingle, S.E. 1999. Sugar metabolism during growth and development in sugarcane Internodes. Crop Science 39: 480-486.

Lingle, S.E. and Smith, R.C. 1991 Sucrose metabolism related to growth and ripening in sugarcane internodes. Crop Science 31: 172–177.

Liu, D.L. and Bull, T.A. 2001. Simulation of biomass and sugar accumulation in sugarcane using a process-based model. Ecological Modeling 144: 181–211.

Liu, D.L., Kingston, G. and Bull, T.A. 1998. A new technique for determining the thermal parameters of phenological development in sugarcane, including suboptimum and supra-optimum temperature regimes. Agricultural and Forest Meteorology 90:119-139.

Malan, C., Baartman, J, Berner, J.M., Patton, A., Hoffman, N., Singels, A. and van Heerden, P.D.R. 2017. Effects of elevated CO_2 on stomatal conductance, biomass partitioning and yield of sugarcane grown in absence of soil water deficit. 2nd Agriculture and Climate Change Congress, 26-28 March 2017, Sitges, Spain. (poster paper)

Pinto, H., Sharwood, R. E., Tissue, D. T. and Ghannoum, O. 2014. Photosynthesis of C3, C3-C4, and C4 grasses at glacial CO_2. Journal of Experimental Botany 65: 3669-3681.

Raes, D., Steduto, P., Hsiao, T.C. and Fereres, E. 2009. AquaCrop - the FAO crop model to simulate yield response to water: II. Main algorithms and software description. Agronomy Journal 101: 438-447.

Rands, R.D. and Dopp, E. 1938. Pythium root rot of sugar cane US Dept Agric Tech Bull 666: 95.

Robertson, M.H., Bonnet, G.D., Hughes, R.M., Muchow, R.C. and Campbell, J.A. 1998. Temperature and leaf area expansion in sugarcane: integration of controlled environment field and model studies. Aust. J. Plant Physiol. 25: 819-828.

Rossler, R.L. 2014. Water Stress Effects on the Growth, Development and Yield of Sugarcane. University of Pretoria, Pretoria, pp. p 124 (M.Sc. Agric. Dissertation).

Ryker, T.C. and Edgerton, C.W. 1931. Studies on sugarcane roots. Louis. Agric. Exp. Sta. Bull. 223: 36.

Sartoris, G.B. 1929. Low temperature injury to stored sugar cane J. Agric. Res. 38: 195-203.

Sinclair, T.R., Gilbert, R.A., Perdomo, R.E., Shine, J.M., Jr. Powell, G. and Montes, G. 2004. Sugarcane leaf area development under field conditions in Florida, USA. Field Crops Research 88: 171-178

Singels, A., Jones, M.R., Marin, F., Ruane, A.C. and Thorburn, P. 2014. Predicting climate change impacts on sugarcane production at sites in Australia, Brazil and South Africa using the Canegro model. Sugar Tech 16(4): 347-355 (also published in Int. Sugar J. 115: 874-881).

Singels, A., Jones, M., van den Berg, M. 2008. DSSAT v4.5 Canegro Sugarcane Plant Module: Scientific documentation. SASRI, Mount Edgecombe, South Africa. pp 34.

Singels, A., Kennedy, A.J. and Bezuidenhout, C.N. 2000. The effect of water stress on sugarcane biomass accumulation and partitioning. Proc S Afr Sug Technol Ass 74: 169-172.

Singels, A., Smit, M.A., and Redshaw, K.A. 2005. The effect of crop start date, crop class and cultivar on sugarcane canopy development and radiation interception. Field Crops Research 92: 249-260.

Singels, A., Van Den Berg, M., Smit, M.A., Jones, M.R. and Van Antwerpen, R. 2010. Modelling water uptake, growth and sucrose accumulation of sugarcane subjected to water stress. Field Crops Research 117: 59-69.

Slabbers, P.J. 1979. Practical prediction of actual evapotranspiration. Irrig. Sci. 1: 185–196.

Smit, M.A., 2010. Characterising the factors that affect germination and emergence in sugarcane. Proc S Afr Sug Technol Ass 83: 230 – 234.

Smit, M.A. and Singels, A. 2006. The response of sugarcane canopy development to water stress. Field Crops Res. 98: 91–97.

Smit, M.A. and Singels, A. 2007. Quantifying the effects of environment and genotype on stalk elongation rate in sugarcane. Proceedings International Society of Sugar Cane Technologists 26, 568-572.

Steduto, P., Hsiao, T.C., and Raes, D. 2009. AquaCrop: The FAO Crop Model to Simulate Yield Response to Water: I: Concepts and Underlying Principles. Agronomy Journal, 101, 426-437.

Stokes, C. J., Inman-Bamber, N. G., Everingham, Y. L., and Sexton, J. 2016. Measuring and modelling CO2 effects on sugarcane. Environmental Modelling & Software 78: 68-78.

Supit, I., Hooijer, A.A., van Diepen, C.A. (Eds.), 1994. System Description of the WOFOST 6.0 Crop Simulation Model Implemented in CGMS. Volume 1: Theory and Algorithms. Joint Research Centre of the European Commission, Luxembourg, Office for Official Publications of the European Communities, EUR 15956, p. 146.

Thornley, J.H.M. and Johnson, I.R. 1990. Plant and Crop Modelling. Oxford University Press, Oxford, UK, p. 669.

Van der Merwe, M.J. and Botha, F.C. 2014. Respiration as a competitive sink for sucrose accumulation in sugarcane culm: Perspective and open questions. In: Physiology, biochemistry and functional biology of sugarcane. (Ed: P.H. Moore and F. C. Botha). 541-571. World in Agriculture Series. Wiley-Blackwell. ISBN 978-1-118-77138-9.

Van Dillewijn C. 1952. Botany of Sugarcane. Chronica Botanica Co.; Waltham, M.A. USA, p. 371.

Vu, J.C.V., Allen, L.H. Jr., and Gesch, R.W. 2006. Up-regulation of photosynthesis and sucrose metabolism enzymes in young expanding leaves of sugarcane under elevated growth CO2. Plant Science 171: 123-131.

Ward, J.K., Tissue, D.T., Thomas, R.B. and Strain, B.R. 1999. Comparative responses of model C3 and C4 plants to drought in low and elevated CO_2. Global Change Biology 5: 857-867.

Webster, A.J., Thorburn, P.J., Roebeling, P.C., Horan, H.L., and Biggs, J.S. 2009. The expected impact of climate change on nitrogen losses from wet tropical sugarcane production in the Great Barrier Reef region. Marine Freshwater Res. 60, 1159–1164.

Zhou, M., Singels, A. and Savage, M.J. 2003. Physiological parameters for modelling differences in canopy development between sugarcane cultivars. Proc S Afr Sug Technol Ass 77:610-621.

APPENDIX B ADDITIONAL CALIBRATION AND VALIDATION RESULTS

The DSSAT-Canegro V4.5_C2.2 model was calibrated using a set of experimental data; model simulation performance for these calibration experiments is shown in Figure B1. The model was then validated by simulating an independent set of experiments, and the performance for these datasets is illustrated in Figure B2.

For the sake of comparing performance between model versions V4.5_C1.1 and V4.5_C2.2, and for consistency with previous publications reporting on Canegro model performance (e.g. Singels and Bezuidenhout, 2002; Singels *et al.*, 2008;), the calibration and validation datasets were pooled and model performance was then evaluated. These results are shown in Figure B3.

The methodology is fully described in the main article.

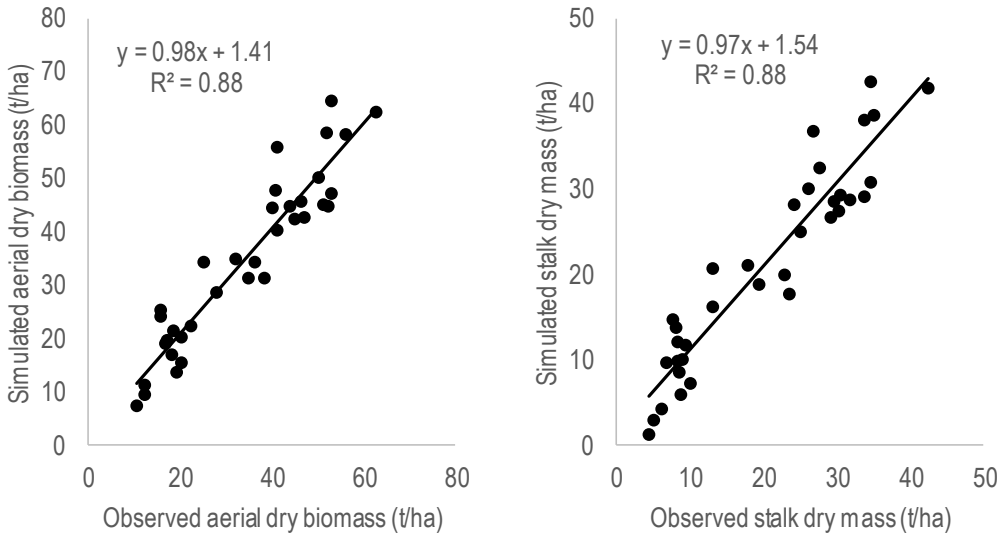

Figure B1. Aerial dry biomass and stalk dry mass, observed and simulated by the DSSAT-Canegro V4.5_C2.2 model for the calibration datasets.

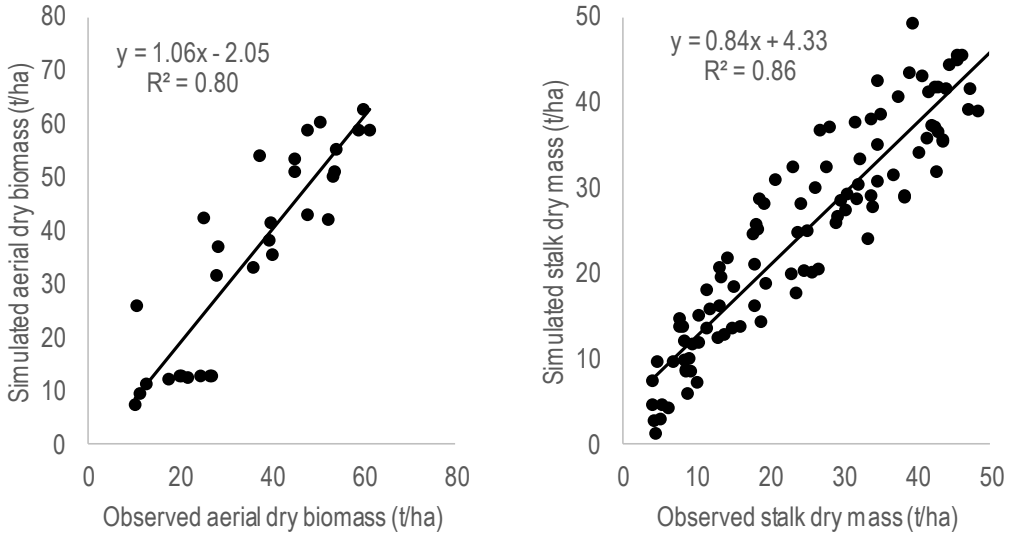

Figure B2. Aerial dry biomass and stalk dry mass , observed and simulated by the calibrated DSSAT-Canegro V4.5_C2.2 model, for the independent validation dataset.

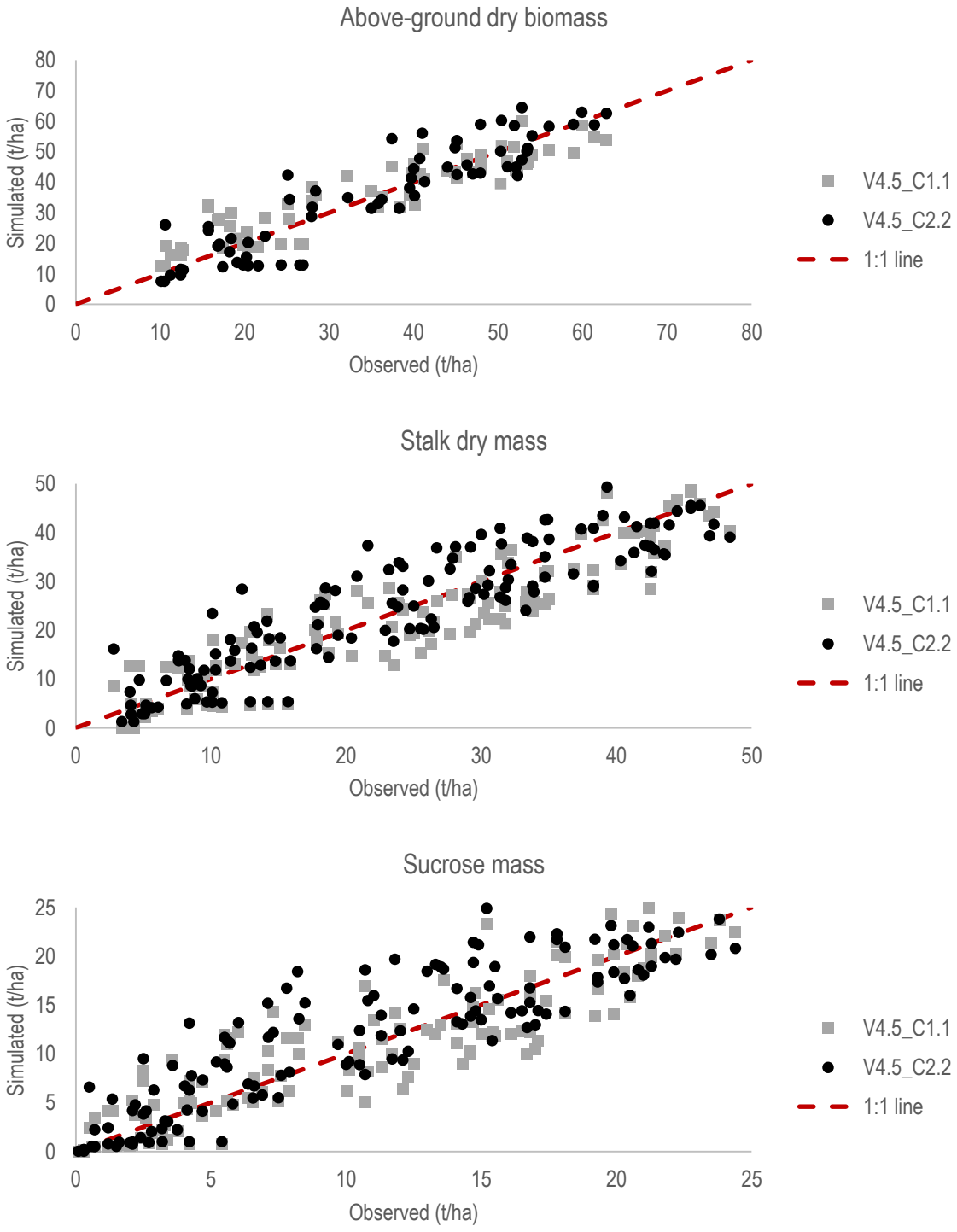

Figure B3. Scatterplots of simulated and observed values of aerial dry mass, stalk dry mass and sucrose mass for cultivars NCo376 for the standard validation dataset simulated by DSSAT-Canegro V4.5_C2.2 and V4.5_C1.1.